Analytica Chimica Acta 788 (2013) 158–164

Contents lists available at SciVerse ScienceDirect

Analytica Chimica Acta

journal homepage: www.elsevier.com/locate/aca

A sensitive DNA biosensor based on a facile sulfamide coupling reaction for capture probe immobilization

Qingxiang Wang[a,*], Yingtao Ding[a], Feng Gao[a], Shulian Jiang[b], Bin Zhang[a], Jiancong Ni[a], Fei Gao[a]

[a] Department of Chemistry and Environment Science, Zhangzhou Normal University, Zhangzhou 363000, PR China
[b] Zhangzhou Product Quality Supervision and Inspection Institute, Zhangzhou 363000, PR China

HIGHLIGHTS

- A versatile sulfonic dye of ANS was electrodeposited on a GCE.
- A DNA biosensor was fabricated based on a facile sulfamide coupling reaction.
- High probe DNA density of 3.18×10^{13} strands cm^{-2} was determined.
- A wide linear range and a low detection limit were obtained.

GRAPHICAL ABSTRACT

A novel DNA biosensor was fabricated through a facile sulfamide coupling reaction between probe DNA and the sulfonic dye of 1-amino-2-naphthol-4-sulfonic acid that electrodeposited on a glassy carbon electrode.

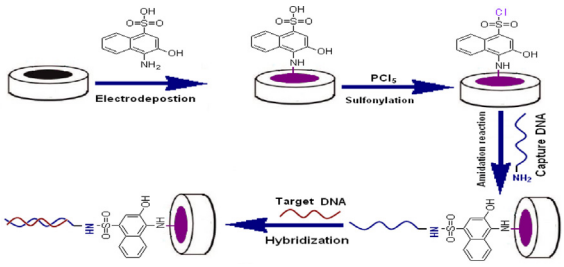

ARTICLE INFO

Article history:
Received 6 April 2013
Received in revised form 5 June 2013
Accepted 17 June 2013
Available online 20 June 2013

Keywords:
DNA biosensor
1-Amino-2-naphthol-4-sulfonic acid
Sulfamide coupling reaction
Electrodeposition

ABSTRACT

A novel DNA biosensor was fabricated through a facile sulfamide coupling reaction. First, the versatile sulfonic dye molecule of 1-amino-2-naphthol-4-sulfonate (AN-SO_3^-) was electrodeposited on the surface of a glassy carbon electrode (GCE) to form a steady and ordered AN-SO_3^- layer. Then the amino-terminated capture probe was covalently grafted to the surface of SO_3^--AN deposited GCE through the sulfamide coupling reaction between the amino groups in the probe DNA and the sulfonic groups in the AN-SO_3^-. The step-by-step modification process was characterized by electrochemistry and attenuated total reflectance Fourier transform infrared (ATR-FTIR) spectroscopy. Using $Ru(NH_3)_6^{3+}$ as probe, the probe density and the hybridization efficiency of the biosensor were determined to be 3.18×10^{13} strands cm^{-2} and 86.5%, respectively. The hybridization performance of the biosensor was examined by differential pulse voltammetry using $Co(phen)_3^{3+/2+}$ (phen = 1,10-phenanthroline) as the indicator. The selectivity experiments showed that the biosensor presented distinguishable response after hybridization with the three-base mismatched, non-complementary and complementary sequences. Under the optimal conditions, the oxidation peak currents of $Co(phen)_3^{3+/2+}$ increased linearly with the logarithm values of the concentration of the complementary sequences in the range from 1.0×10^{-13} M to 1.0×10^{-8} M with a regression coefficient of 0.9961. The detection limit was estimated to be 7.2×10^{-14} M based on 3σ.

1. Introduction

With the development of biotechnology and medicine, simple, fast and sensitive detection of target DNA provides promising potential in forensic, clinical and pharmaceutical applications [1,2]. So far, various methods have been developed for DNA detection,

* Corresponding author. Tel.: +86 596 2591445; fax: +86 596 2520035.
E-mail address: axiang236@126.com (Q. Wang).

0003-2670/$ – see front matter © 2013 Elsevier B.V. All rights reserved.
http://dx.doi.org/10.1016/j.aca.2013.06.018

such as fluorescence, surface plasmon resonance spectroscopy, electrochemistry and quartz crystal microbalance [3–5]. Among these, the electrochemical methods, mainly based on DNA electrochemical biosensors, attract considerable interest owing to their advantages of simplicity, low-cost, high selectivity and high sensitivity [6–9]. The basic step for fabricating an electrochemical biosensor is the immobilization of DNA probes on the transducer surface, which is found to be the most crucial part to decide the sensitivity, accuracy and stability of the DNA biosensor [3,10,11].

To date, many strategies, such as physical absorption [12], electrostatic binding [13], self-assembly [14], biotin–streptavidin interaction [15] and covalent coupling [16] have been developed for probing DNA immobilization. Thereinto, the covalent method based on the coupling reaction of the probe DNA with the functional groups on the surface of the transducer receives much attention since it provides a stable sensing interface preventing probe DNA desorption from the electrode surface [17]. Moreover, the covalent method usually results in high hybridization efficiency because in this way the loading density, structural flexibility and orientation control of the probe chains are often well assured [18]. Currently, the used covalent reactions for probe DNA immobilization include the condensation reactions between the 5′ $-PO_4^{3-}$ of DNA and the —COOH, —OH, $-NH_2$ confined on the transducer or the coupling between the $-NH_2$ modified on probe DNA terminal and the derivate —COOH [19–21] on the transducer. However, in order to obtain the success of these condensation reactions, the 1-ethyl-3-(3-dimethylaminopropyl) carbodiimide hydrochloride (EDC) that is usually used in conjunction with N-hydroxysuccinimide (NHS) is often applied to pre-activate the groups of —COOH or $-PO_4^{3-}$. But this procedure makes the whole experimental processes more cumbersome. What is more, the high price and easy deliquescence feature of these reagents lead to the increase of the fabricating cost of the biosensor.

The sulfamide coupling reaction between amino and sulfonic group is a type of typical condensation reaction in organic synthesis. Although compared with the carbodiimide-based condensation reaction mentioned above, the sulfamide coupling reaction is carried out in a non aqueous medium [22,23], the merits including mild reaction condition and readily available activating reagent (PCl_5) still make this type of reaction possessing great promising in bioconjunction field. Chen et al. [22] have immobilized the amino modified locked nucleic acid (LNA) on a glassy carbon electrode (GCE) modified with *p*-aminobenzenesulfonic acid (*p*ABS). The results showed that the biosensor developed in this way presented good stability and excellent hybridization performance. More recently, Hu et al. [23] have also used the isomer of *p*ABS, *m*-aminobenzenesulfonic acid (*m*ABS) as the sulfonic group source to obtain a $-SO_3^-$ coated TiO_2 nanosheet surface, and then coupled with the amino terminated DNA for biosensor construction. However, to the best of our knowledge, the other sulfonic acid-based dyes have not been applied as modified materials for DNA immobilization yet, although this type of dyes is very convenient to synthesize.

The compound 1-amino-2-naphthol-4-sulfonic acid (AN-SO_3^-) is a typical sulfonic acid dye, which has widespread applications in the fields of chemistry and industry since it has multiple functional groups (—OH, $-SO_3H$ and $-NH_2$). For example, it has been applied as the substrate for the indirect determination of iodide ion [24], Mo(VI) [25], phosphorus [26], owing to its reducing property. It has also been used as the monomer to synthesize the conductive polymer or as the dopant to prepare the copolymer with aniline [27]. Additionally, Ćirić-Marjanovića et al. [28] reported that the electrochemically oxidized product of AN-SO_3^- shows good semiconductivity due to unpaired electrons structure, which make the dye possessing great potential in electroanalytical field.

In this work, a novel and high performance biosensor was fabricated based on the sulfamide coupling reaction between the sulfonic groups in AN-SO_3^- and the amino groups in the modified probe DNA. Firstly, the AN-SO_3^- molecule was electrodeposited on a GCE through electro-oxidizing the amino group on AN-SO_3^- at a high potential range [29]. After converting the sulfonic groups to the active sulfonyl chloride by PCl_5, the amino modified probe DNA was grafted on electrode surface via a sulfamide coupling reaction. Characterization experiments indicated that the biosensor has large probe DNA loading density and high hybridization efficiency. Analytical tests further showed that when a classical DNA structure discriminator $Co(phen)_3^{3+/2+}$ (phen = 1,10-phenanthroline) was used as the electrochemical hybridization indicator, the complementary target DNA could be detected in a wide concentration range from 1.0×10^{-13} M to 1.0×10^{-8} M. Good regeneration ability and reproducibility could also be achieved for the biosensor. This work brings a promising application of sulfonic dyes in biosensor preparation.

2. Experimental

2.1. Reagents

1-Amino-2-naphthol-4-sulfonic acid (AN-SO_3^-) was of analytical grade and purchased from Jinshan Ting New Chemical Reagent Factory (China). The hybridization indicator of $Co(phen)_3^{3+/2+}$ was synthesized and purified according to literature [30]. Hexaammineruthenium(III) chloride ($[Ru(NH_3)_6]^{3+}$) was purchased from ABCR GmbH & Co. KG (Germany). Phosphorus pentachloride (PCl_5) was obtained from Aladdin Reagent Co., Ltd. (China). Phosphate buffer solution (PBS) was provided by Shanghai Kang-Yi Instruments Co., Ltd. (China). All the other chemicals were of analytical reagent grades and the deionized water was used throughout in this paper.

The 18-mer oligonucleotides from cauliflower mosaic virus (CaMV) 35S promoter gene were synthesized by Shanghai Sangon Biotechnology Co., Ltd. (China). Their base sequences were as follows:

- Capture probe sequence (S1): 5′-NH_2-$(CH_2)_6$-TCT TTG GGA CCA CTG TCG-3′
- Complementary sequence (S2): 5′-CGA CAG TGG TCC CAA AGA-3′
- Three-base mismatched sequence (S3): 5′-CGA CAA TGG CCC CAA CGA-3′
- Non-complementary sequence (S4): 5′-GCA TCG AGC GAG CAG GTA-3′

Stock solutions (10 μM) of all the oligonucleotides were prepared with TE butter solution (10 mM Tris–HCl, 1.0 mM EDTA, pH 8.0) and kept frozen.

2.2. Apparatus

Attenuated total reflectance-Fourier transform infrared spectroscopy (ATR-FTIR) was recorded on a NICOLET iS10 IR optical spectrometer (Thermo Fisher Scientific Inc., Madison, WI, USA). Electrochemical experiments including cyclic voltammetry (CV), differential pulse voltammetry (DPV), chronocoulometry (CC) and electrochemical impedance spectroscopy (EIS) were measured on a CHI 650C electrochemical analyzer (Shanghai CH Instrument, China). A conventional three-electrode system was used with a modified glassy carbon working electrode, a platinum wire auxiliary electrode and an Ag/AgCl/(3 M KCl) reference electrode. The hybridization temperature was controlled by Water Bath Constant Temperature Oscillator (China).

2.3. Procedures

2.3.1. Electrodeposition of AN-SO_3^- on GCE

Before deposition with AN-SO_3^-, the GCE surface was first polished to a mirror like finish with 1.0, 0.3 and 0.05 μm alumina sequentially, and then sonicated respectively in acetone, ethanol and water for 2 min.

The AN-SO_3^- coated GCE was prepared according to the following procedures: the cleaned GCE was immersed into a 10 mL cell that containing 10 mM AN-SO_3^- and 25 mM PBS (pH 7.0), and then CV scanned between +1.5 V and −0.5 V with the scan rate of 20 mV s^{-1} until the steady CV curves appeared. Afterwards, the electrode was immersed in deionized water for 5 min with shaking to remove the physically absorbed AN-SO_3^- molecules. Thus, an AN-SO_3^- modified electrode (SO_3^--AN/GCE) was obtained.

2.3.2. Covalent immobilization of probe DNA on the SO_3^--AN/GCE and the hybridization reaction

To immobilize probe DNA (S1) on SO_3^--AN/GCE, the SO_3^--AN/GCE was first immersed into 2 mL acetone containing 0.04 M PCl_5 for 30 min to transfer the sulfonic groups to the sulfonyl groups [22,23], thus the sulfonylated AN-SO_3^- modified electrode ($ClSO_2$-AN/GCE) was obtained. Then a drop (10 μL) of 1.0 μM amino modified probe sequence (S1) was placed on the modified electrode for sulfanilamide coupling reaction. After natural drying and rinsed with TE buffer solution, the probe DNA modified electrode was obtained, which was denoted as S1-NH-SO_2-AN/GCE.

The hybridization reactions of the biosensor with the target sequences (S2) were performed by incubating S1-NH-SO_2-AN/GCE into the hybridization solution containing the desired concentration of target sequences at 42 °C for 45 min. After successively washes with TE buffer and deionized water to remove the unhybridized DNA, the hybridized electrode was obtained. The hybridization selectivity of the biosensor was investigated through hybridization with the three-base mismatched (S3) and non-complementary (S4) sequences, respectively. The brief procedures for preparation of the biosensor are illustrated in Fig. 1.

2.4. Electrochemical measurements

2.4.1. Electrochemical characterization of the modified electrodes

The step-by-step modification process of the biosensor was electrochemically characterized by CV and EIS using the mixture of 5.0 mM $Fe(CN)_6^{3-/4-}$ and 0.1 M KCl as the redox probe. The scan rate in CV was 100 mV s^{-1}, and the scan potential was varied in the range from +0.6 V to −0.3 V. The EIS was collected at a potential of +0.23 V in the frequency range from 0.05 to 10^4 Hz with the voltage amplitude of 5 mV.

2.4.2. Hybridization detection with $Co(phen)_3^{3+/2+}$ as the electroactive indicator

Before measurements, S1-NH-SO_2-AN/GCE or its hybridized electrodes were immersed into a stirring solution containing 0.1 mM $Co(phen)_3^{3+/2+}$ and 0.1 M KCl for 10 min for binding equilibrium and then measured in 0.1 M KCl solution with CV or DPV after rinsing with water. The CV was scanned from +0.6 V to −0.3 V, and the DPV was scanned in the potential range from −0.2 V to +0.4 V with an amplitude of 5 mV.

2.4.3. DNA surface density and hybridization efficiency determination

The DNA surface density was determined using a typical CC method that has been reported by Steel et al. [31]. It is accorded that $[Ru(NH_3)_6]^{3+}$ cations as counter ions can bind to anionic phosphate of DNA strands in a stoichiometric approach, thereby allowing the quantitative analysis of the loading amount of DNA. In the experiment, the charge (Q), as a function of time (t) is given by the following integrated Cottrell expression:

$$Q = \frac{2nFAD_0^{1/2}C_0^*}{\pi^{1/2}}t^{1/2} + Q_{dl} + nFA\Gamma_0 \quad (1)$$

where n is the number of electrons per molecule for reduction, F the Faraday constant (C mol^{-1}), A the electrode area (cm^2), D_0 the diffusion coefficient (cm^2 s^{-1}), C_0^* the bulk concentration (mol cm^{-2}), Q_{dl} the capacitive charge (C), and $nFA\Gamma_0$ is the charge from the reduction of adsorbed redox markers. The intercept at $t = 0$ is the sum of the double layer charging and the surface excess terms. Then when the double layer capacitance is assumed to be approximately

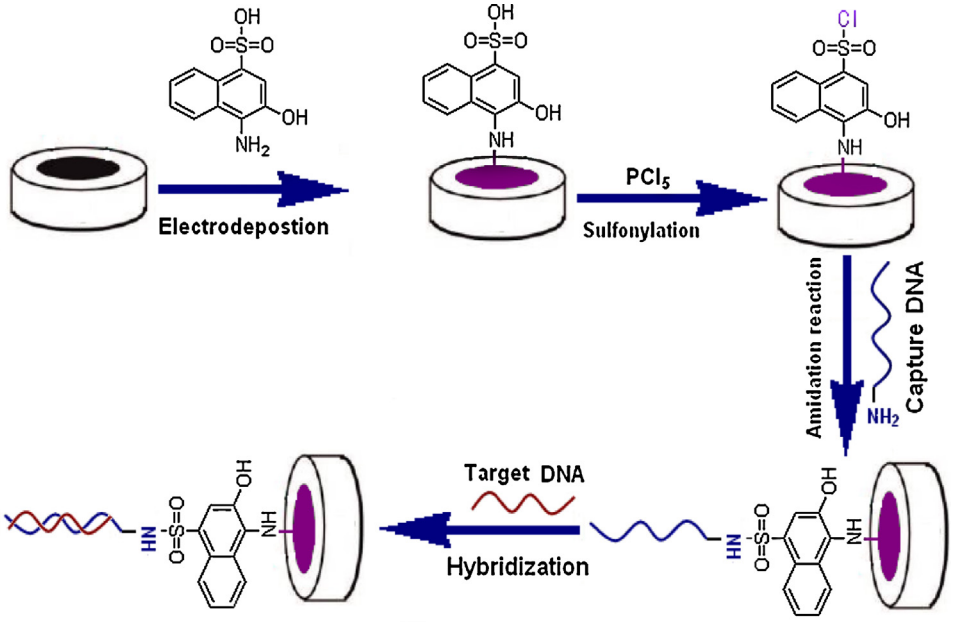

Fig. 1. Diagram of the fabrication and hybridization procedure the DNA biosensor.

equal in measurements with and without $[Ru(NH_3)_6]^{3+}$ [31] and Q_{dl} for the fixed voltage step is constant, $nFA\Gamma_0$ can be achieved by measuring the difference in intercepts of the two cases, and the DNA surface density can be further determined by the following equation:

$$\Gamma_{DNA} = \Gamma_0 \left(\frac{z}{m}\right) N_A \quad (2)$$

where Γ_{DNA} is the probe surface density (strands cm^{-2}), m the number of phosphate groups on the probe DNA, z the charge on the redox molecule, and N_A the Avogadro's number.

3. Results and discussion

3.1. Electrodeposition of AN-SO_3^- on GCE surface

Since Barbier et al. [29] first reported that the amine-containing compounds could be electro-oxidized to amine cation radical at high potential and subsequently form a carbon–nitrogen linkage on the carbon surface, a new way to construct monolayer film on carbon-based electrode was opened. In this work, the immobilization of AN-SO_3^- on GCE was also achieved by the electrodeposition method. Fig. 2 shows the repetitive CVs of 10 mM AN-SO_3^- solution on the bare GCE electrode with the scan rate of 20 mV s^{-1}. It was observed that between the potential range of −0.5 V and +1.5 V, two weak reduction peaks were occurred at +0.43 V (P1) and −0.18 V (P2), respectively, accompanied by a wide oxidation peak (P3) at +0.95 V, which indicated that the electrochemical process of AN-SO_3^- on GCE surface was irreversible. According to previous investigations on the electrochemistry of amino-compounds, the oxidation peak at +0.95 V could be ascribed to the oxidation of the amino group to its cation radical [32,33]. With the increase of the sweep cycles, all the peaks decreased gradually, suggesting the continuous growth of the AN-SO_3^- film on GCE. When the sweep cycles were more than five, all the peaks were hardly changed, demonstrating that a saturated deposition layer of AN-SO_3^- had been formed on the GCE. Additionally, it was found that when the electrochemical deposition process was finished, the surface of GCE was changed from the shiny black to the uniform blackish-brown, further indicating that AN-SO_3^- had been successfully deposited on the surface of the GCE.

3.2. ATR-FTIR and electrochemical characterization of the biosensor

The fabrication process of the biosensor was characterized by ATR-FTIR and electrochemical methods. The ATR-FTIR spectra of

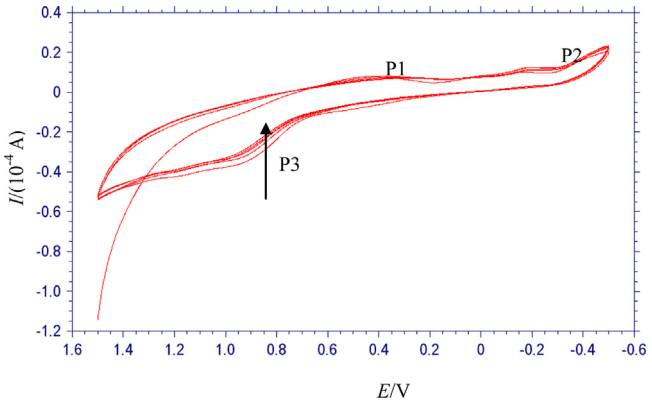

Fig. 2. Cyclic voltammograms of polymerization of AN-SO_3^- (10 mM) in 25 mM PBS (pH 7.0) on the glassy carbon electrode in the potential range from −0.5 to +1.5 V at a scan rate of 20 mV s^{-1}.

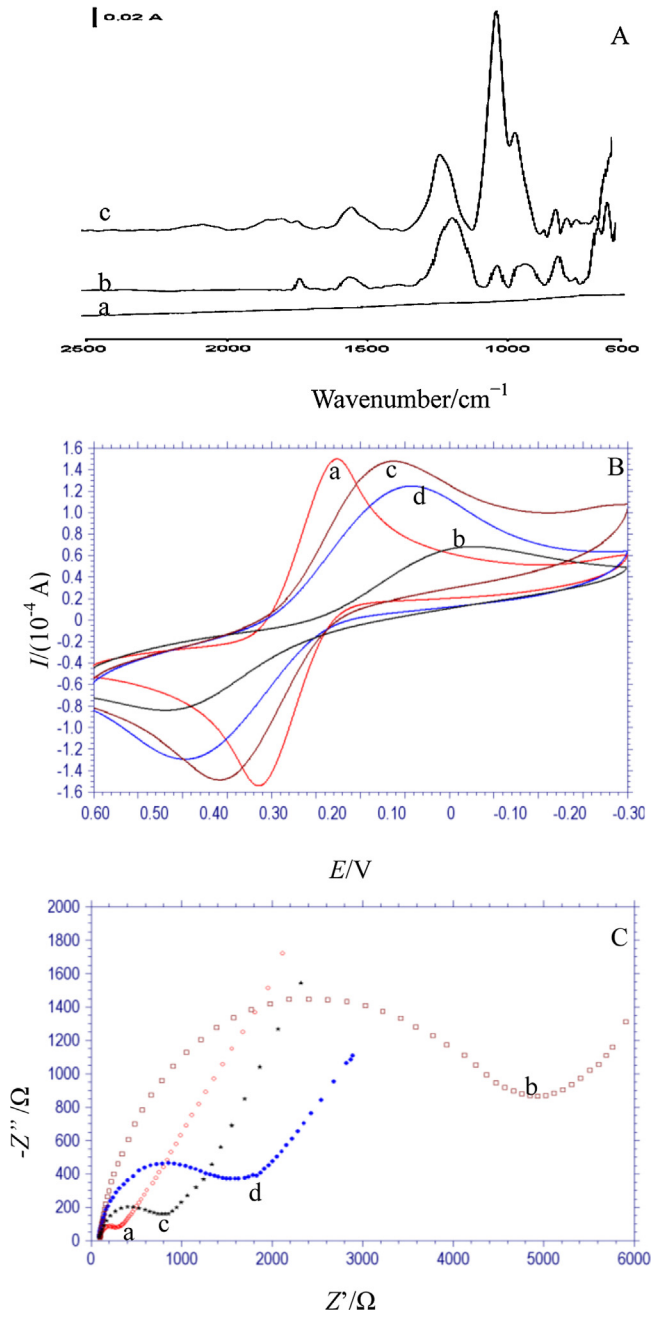

Fig. 3. (A) ATR-FTIR spectra of bare GCE (a), SO_3^--AN/GCE (b) and S1-NH-SO_2-AN/GCE (c); (B) cyclic voltammograms and (C) Nyquist plots of 5.0 mM $Fe(CN)_6^{3-/4-}$ (1:1) in 0.1 M KCl recorded on bare GCE (a), SO_3^--AN/GCE (b), $ClSO_2$-AN/GCE (c) and S1-NH-SO_2-AN/GCE (d).

the different electrodes were showed in Fig. 3A. It was observed that bare GCE did not produce any significant features in the spectra (curve a). However on SO_3^--AN/GCE (curve b), some bands that were in consistent with the characteristic absorption of free AN-SO_3^- were observed [24]: The absorption peak occurred at 1567 cm^{-1} could be ascribed to C=C stretching vibration of the aromatic ring. The aromatic C—H out-of-plane bending vibrations for four adjacent hydrogen atoms in the disubstituted benzene ring were observed around 833 cm^{-1}. The other two bands at 1230 cm^{-1} and 1038 cm^{-1} belonged to the characteristic stretching absorption of —OH and SO_3^-, respectively. These functional groups in the ATR-FTIR spectra also confirmed that AN-SO_3^- had been anchored on the surface of GCE. Upon further grafting with probe

DNA (curve c), it was found that a sharply increased peak ascribing to the characteristic absorption of DNA phosphodiester bond appeared at 1033 cm^{-1} [34]. Also a new broad band corresponded to the exocyclic $-NH_2$ and the purine/pyrimidine rings [35] were observed from 1767 cm^{-1} to 1875 cm^{-1}. These variations suggested that the probe DNA had been successfully grafted on the electrode surface.

The CV and EIS techniques were also applied to characterize the step-by-step assembly process of the biosensor. Fig. 3B shows the CVs of 5.0 mM $Fe(CN)_6^{3-/4-}$ with 0.1 M KCl on bare GCE (curve a), SO_3^--AN/GCE (curve b), $ClSO_2$-AN/GCE (curve c) and S1-NH-SO_2-AN/GCE (curve d). It could be clearly seen that a pair of well-defined redox peaks corresponding to the electrochemical process of the $Fe(CN)_6^{3-/4-}$ couple were occurred on the bare GCE. However on SO_3^--AN/GCE, the redox peaks decreased dramatically in comparison with those of on bare GCE, which suggested that the deposited AN-SO_3^- layer significantly blocked the electron transfer process of $Fe(CN)_6^{3-/4-}$ ions on the electrode surface due to the electrostatic repulsion force. However, when the SO_3^--AN/GCE was treated with PCl_5, it was found that the redox peaks of $Fe(CN)_6^{3-/4-}$ ions increased greatly. This can be explained by the following reasons: (1) when the negatively charged sulfuric groups on the electrode surface were converted to the neutral sulfonyl groups, the $Fe(CN)_6^{3-/4-}$ can feasibly diffuse to the electrode surface; (2) the electrodeposition product has been proved to have semiconductivity due to the existence of unpaired electrons [28], which allows the electroactive probe to transfer electrons easily to the modified electrode. Further, when the acylated electrode of $ClSO_2$-AN/GCE was grafted with the probe DNA, the redox peaks of $Fe(CN)_6^{3-/4-}$ decreased again, which can be ascribed to the electrostatic repulsion of phosphate backbone on DNA toward the $Fe(CN)_6^{3-/4-}$ ions. This also means that the DNA probe has been successfully anchored on the electrode by the designed protocol.

The corresponding Nyquist diagrams of $Fe(CN)_6^{3-/4-}$ on the different electrtodes were depicted in Fig. 3C. It was observed that the semicircle diameter that often reflected the electron transfer resistance (R_{et}) was small on bare GCE (R_{et} = 200 Ω, curve a). But on SO_3^--AN/GCE, the electron transfer resistance increased significantly (R_{et} = 4600 Ω, curve b), also suggesting that AN-SO_3^- has been deposited on GCE and blocked the approaching of $Fe(CN)_6^{3-/4-}$ to the electrode surface. However on $ClSO_2$-AN/GCE, the semicircle diameter corresponding to the electron transfer resistance was decreased to 720 Ω (curve c), suggesting the electron transfer resistance on SO_3^--AN/GCE was decreased by the acylation, and this result was well in consistent with the above CV results. Also when the probe DNA was grafted, the R_{et} value was increased again owing to the electrostatic resistance between negatively charged DNA and $Fe(CN)_6^{3-/4-}$ ions.

It was also noticeable that the surface coverage (θ) of AN-SO_3^- on GCE was calculated to be 95.65% in terms of the following equation [36]:

$$\theta = 1 - \frac{R_{et}^{bare}}{R_{et}^{AN}} \quad (3)$$

where R_{et}^{bare} and R_{et}^{AN} are the electron transfer resistances of $Fe(CN)_6^{3-/4-}$ on bare GCE and SO_3^--AN/GCE, respectively.

The sufficiently large θ value also suggested that the GCE surface had been well covered by a layer of AN-SO_3^- molecules.

3.3. Determination of DNA surface density and hybridization efficiency

We had also determined DNA immobilization density on electrode surface by CC method that has been reported by Steel and co-workers [31]. First, the concentration of $[Ru(NH_3)_6]^{3+}$ probe used in this experiment was optimized, and the results showed that the total charge obtained from the CC curves increased as higher concentrations of $[Ru(NH_3)_6]^{3+}$. When the concentration of $[Ru(NH_3)_6]^{3+}$ increased to 1.0×10^{-4} M, the CC curve become stable. Therefore, 1.0×10^{-4} M $[Ru(NH_3)_6]^{3+}$ was adopted for the following experiment. Fig. 4 shows the typical CC curves of S1-NH-SO_2-AN/GCE in Tris–HCl buffer solution without (curve a) and with 1.0×10^{-4} M $[Ru(NH_3)_6]^{3+}$ (curve b), and S2 hybridized electrode in Tris–HCl buffer solution containing 1.0×10^{-4} M $[Ru(NH_3)_6]^{3+}$ (curve c). From the figure, it could be found that the intercept increased in the order of hybridized electrode in $[Ru(NH_3)_6]^{3+}$ solution, S1-NH-SO_2-AN/GCE in $[Ru(NH_3)_6]^{3+}$ solution, and S1-NH-SO_2-AN/GCE in blank Tris–HCl buffer solution.

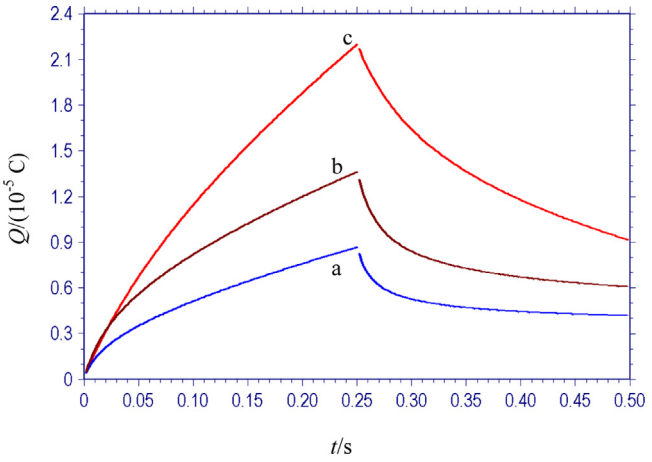

Fig. 4. Chronocoulometric curves for probe DNA modified electrode in the absence (a) and presence of 1.0×10^{-4} M $[Ru(NH_3)_6]^{3+}$, (b) and hybridized with 1 μM complementary DNA in the presence of 1.0×10^{-4} M $[Ru(NH_3)_6]^{3+}$ (c). The CC is carried out at a potential range between 0.05 V and −0.45 V and a pulse width of 0.25 s. The electrolyte solution is 20 mM Tris–HCl buffer solution.

Then, from the intercept difference of $Q \sim t^{1/2}$ between curve b and curve a, the value of $nFA\Gamma_0$ corresponding to the electroactive $[Ru(NH_3)_6]^{3+}$ electrostatically bound to the probe DNA was determined to be 3.82 μC. Then from the CV data in Fig. 3, the electrode surface (A) was determined to be 0.124 cm^2 according to the Randles–Sevcik expression: $I_p = 2.69 \times 10^5 AD^{1/2}n^{3/2}Cv^{1/2}$, where D represents the diffusion coefficient of the electroactive molecules in solution ($[6.70 \pm 0.02] \times 10^{-6}$ cm^2 s^{-2}), n the number of electrons participating in electrode reaction, C the concentration of the probe molecule (5.0 mM), and v the scan rate (100 mV s^{-1}).

Thus, based on Eq. (2), the value of Γ_{DNA} was determined to be 3.18×10^{13} strands cm^{-2}, which is comparable with gold nanoparticle modified electrode [37], and this also demonstrated that the AN-SO_3^- monolayer-based electrode had considerably high success for DNA immobilization. In addition, when a maximum limiting amount (1 μM) of S2 was hybridized, the total density of DNA was determined to be 5.93×10^{13} strands cm^{-2} by the similar procedure, suggesting that the hybridization efficiency of 86.5% was obtained for the developed DNA biosensor, which is higher than the reported values in literatures [31,38]. This was likely ascribed to the following two reasons: (1) compared with the immobilization platform presented in literatures [17,18], the AN-SO_3^- molecule with large naphthol ring was applied as a substrate for DNA immobilization, which made the adjacent probe strands having enough space for the target DNA to access for hybridization and (2) the —OH on the naphthalene ring of AN-SO_3^- effectively prevent the immobilized DNA from lying flat on the electrode surface, allowing the probe DNA to keep a good orientation for hybridization reaction.

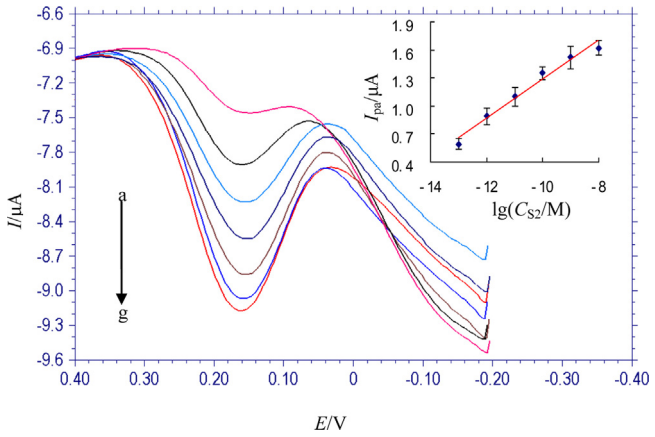

Fig. 5. Differential pulse voltammograms (DPVs) of 0.1 mM $Co(phen)_3^{3+/2+}$ accumulated on S1-NH-SO_2-AN/GCE before (a) and after its hybridization with 1.0×10^{-13} M (b), 1.0×10^{-12} M (c), 1.0×10^{-11} M (d), 1.0×10^{-10} M (e), 1.0×10^{-9} M (f), 1.0×10^{-8} M (g). Inset shows the plot of the oxidation peak currents versus the logarithm value of S2. The DPV is scanned in the potential range from −0.2 V to +0.4 V with an amplitude of 5 mV and the electrolyte solution is 0.1 M KCl.

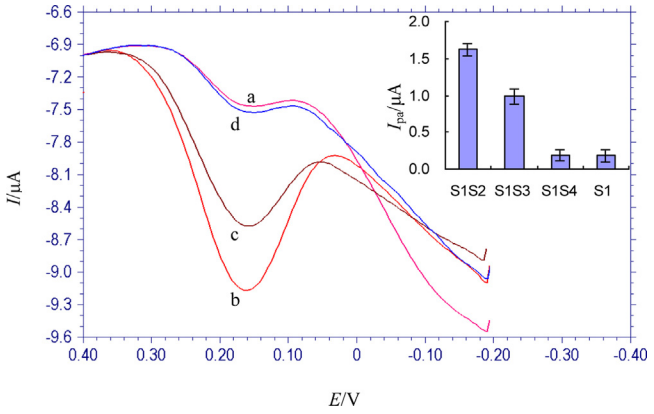

Fig. 6. DPVs of 0.1 mM $Co(phen)_3^{3+/2+}$ recorded on S1-NH-SO_2-AN/GCE (a) and its hybridization with complementary sequences S2 (b), three-base mismatched sequences S3 (c) and non-complementary sequences S4 (d). Inset shows the bar graph of the peak current values of $Co(phen)_3^{3+/2+}$ with different sequences. The concentrations for all the hybridized sequences were 1.0×10^{-8} M. The DPVs were scanned in the potential range from −0.2 V to +0.4 V with an amplitude of 5 mV and the electrolyte solution is 0.1 M KCl.

3.4. Detection of sequence-specific DNA fragment

It has been well known that the electroactive $Co(phen)_3^{3+/2+}$ compound interacts in different ways with ssDNA and dsDNA, and is often used as an electrochemical probe for monitoring the hybridization process [39,40]. In this work, $Co(phen)_3^{3+/2+}$ was also applied as a hybridization indicator for the detection of target sequences. The electrochemical responses of $Co(phen)_3^{3+/2+}$ on S1-NH-SO_2-AN/GCE and its hybridized electrode were displayed in Fig. S1 in Supplementary material. It was found that on S1-NH-SO_2-AN/GCE, only a pair of very small redox peaks with the oxidation peak current (I_{pa}) of 0.08 μA were observed (curve a in Fig. S1), but after hybridization with 1.0×10^{-8} M target DNA (S2), the redox peaks were increased moderately, and the oxidation peak current was increased to 0.1 μA (curve b in Fig. S1), proving that the electroactive probe of $Co(phen)_3^{3+/2+}$ was also appropriate for indicating the hybridization process in the developed biosensor. In addition, with the increase of scan rate (ν), the electrochemical signals of $Co(phen)_3^{3+/2+}$ on the hybridized electrode increased accordingly (see Fig. S2 in Supplementary material), and the oxidation peak currents (I_{pa}) shows a good linearity with ν in the range from 10 mV s^{-1} to 280 mV s^{-1} with a linear regression equation of $I_{pa}/\mu A = 13.65\,\nu/(V\,s^{-1}) + 1.86$ ($r = 0.994$) (inset of Fig. S2), suggesting that the electrochemical behaviors of $Co(phen)_3^{3+/2+}$ is controlled by an adsorption process. According to the references of [39,40], the adsorption process can be explained by the specific intercalation of $Co(phen)_3^{3+/2+}$ into the adjacent base pairs of the hybridized duplex DNA.

The DPV measurements of $Co(phen)_3^{3+/2+}$ oxidation on S1-NH-SO_2-AN/GCE hybridization with various concentrations of target sequences were applied to investigate the dynamic range and detection limit of the developed biosensor. The obtained DPV curves were showed in Fig. 5. It could be found that the oxidation peaks of $Co(phen)_3^{3+/2+}$ increased with the increase of S2 concentrations (C_{S2}), demonstrating that more and more duplex had been formed on the biosensor through the hybridization reaction. The oxidation peak currents (I_{pa}) presented a good linear relationship with the logarithm of C_{S2} ($\log C_{S2}$) in the range from 1.0×10^{-13} M to 1.0×10^{-8} M (inset of Fig. 5). The regression equation was I_{pa} (μA) = 0.208 log(C_{S2}/M) + 3.36 with a correlation coefficient (r) of 0.9961. When the hybridization buffer solution without S2 was applied as the blank solution, a detection limit of 7.2×10^{-14} M was estimated based on 3σ (where σ is the standard deviation of the blank solution, $n = 7$).

The hybridization selectivity of the developed DNA biosensor was further evaluated by hybridizating S1-NH-SO_2-AN/GCE with different kinds of DNA fragments, including the complementary sequences (S2), the three-base mismatched sequences (S3), and the non-complementary sequences (S4). Fig. 6 shows the DPVs of $Co(phen)_3^{3+/2+}$ on S1-NH-SO_2-AN/GCE before (curve a) and after hybridization with the same concentrations (1.0×10^{-8} M) of S2 (curve b), S3 (curve c) and S4 (curve d), and the corresponding bar graph was depicted in inset of Fig. 6. As seen, the highest DPV signal was obtained on S2 hybridized electrode because the intact duplex structure was formed between S2 and S1, resulting in the largest binding of $Co(phen)_3^{3+/2+}$ to the electrode surface. As expected, no significant difference of the oxidation peak was observed between S1-NH-SO_2-AN/GCE and S4 hybridized electrode, suggesting that the hybridization event between S1 and S4 did not happen. These results showed that the developed biosensor had good hybridization selectivity to discriminate the complementary sequences from the non-complementary ones. However, when the biosensor was hybridized with the three-base mismatched sequences of S3, the local duplex structure was formed on the biosensing interface, and some indicators was adsorbed on the electrode surface by intercalation into the local duplex sites, resulting in a relatively high oxidation peak (curve c). This leaded to the difficulty to distinguish the target DNA with low concentration from the three-mismatched DNA with high concentration. Therefore it is still a challenge to exploit good way that can transform the hybridization event into the readable signal more accurately.

3.5. Regeneration, reproducibility and stability of the DNA biosensor

The reusability of a biosensor is extremely important for practical applications. In this work, the regeneration ability of the biosensor was investigated through the following procedures: the fabricated biosensor was immersed into a hybridization solution containing 1.0×10^{-8} M S2 for 45 min and then incubated in $Co(phen)_3^{3+/2+}$ for 10 min. After the electrochemical measurements, the DNA biosensor was regenerated by incubating in a buffer solution at 90 °C for 10 min and then cooled with ice-water. The results showed that by such a routine, the biosensor could be successively used for at least five times without loosing

its hybridization ability (Fig. S3 in Supplementary material). This excellent performance was likely related to the co-contributions from the steady electrodeposition film of AN-SO_3^- on GCE and the tight sulfamide bond between the probe DNA and the electrode surface.

The reproducibility of the DNA biosensor was also measured by a parallel assay. Three parallel-made DNA sensors were used to detect 1.0×10^{-8} M target DNA sequence, and the obtained peak currents of $Co(phen)_3^{3+/2+}$ were 1.70 μA, 1.67 μA, 1.52 μA, respectively. The relative standard deviation (RSD) was determined to be 7.9%, which indicated that the reproducibility of the developed DNA biosensor was satisfactory. In addition, the stability experiments showed that after a fabricated biosensor was stored at 4 °C in a dry state for 20 days, the obtained hybridization response was very close to that before storage (Fig. S4 in Supplementary material), indicating that the developed biosensor had high stability.

4. Conclusions

In this paper, a layer of AN-SO_3^- molecules was electrodeposited on a glassy carbon electrode by cyclic voltammetry, and a DNA biosensor was further constructed based on a facile condensation reaction between the sulfonic groups of the deposited AN-SO_3^- and the modified amino on probe DNA. Using $Ru(NH_3)_6^{3+}$ as an electroactive probe, the probe density and the hybridization efficiency of the prepared biosensor were determined to be 3.18×10^{13} strands cm^{-2} and 86.5%, respectively. In the detection of 18-mer synthetic oligonucleotides from CaMV 35S promoter gene, the biosensor presented different electrochemical response after hybridization with three-base mismatched, non-complementary and complementary sequences. The target sequences could be detected in a concentration range from 1.0×10^{-13} M to 1.0×10^{-8} M with a detection limit of 7.2×10^{-14} M. Additionally, because the probe DNA was immobilized on the electrode surface by a tight covalent bond, the biosensor shows good stability and regeneration.

Acknowledgment

The work is supported by the NSFC (No. 21275127), Key Research Foundation of Fujian Education Department (No. JA11166), Natural Science Foundation of Fujian Province (No. 2011J01059), Program for New Century Excellent Talents in Fujian Province University (No. JA12204), Science and Technology Project of SIQSAQ (No. 2011QK217) and Key Provincial University Project of Fujian (No. JK2011032).

Appendix A. Supplementary data

Supplementary data associated with this article can be found, in the online version, at http://dx.doi.org/10.1016/j.aca.2013.06.018.

References

[1] A. Vorsters, I. Micalessi, J. Bilcke, M. Ieven, J. Bogers, P. Van Damme, Eur. J. Clin. Microbiol. 31 (2012) 627–640.
[2] J. Berganza, G. Olabarria, R. García, D. Verdoy, A. Rebollo, S. Arana, Biosens. Bioelectron. 22 (2007) 2132–2137.
[3] A. Sassolas, B.D. Leca-Bouvier, L.J. Blum, Chem. Rev. 108 (2008) 109–139.
[4] Y. Yang, L. Zhao, Trends Anal. Chem. 29 (2010) 980–1003.
[5] J.E.N. Dolatabadi, O. Mashinchian, B. Ayoubi, A.A. Jamali, A. Mobed, D. Losic, Y. Omidi, M. de la Guardia, Trends Anal. Chem. 30 (2011) 459–472.
[6] J. Liu, X. Yuan, Q. Gao, H. Qi, C. Zhang, Sens. Actuators B: Chem. 162 (2012) 384–390.
[7] F. Lucarelli, S. Tombelli, M. Minunni, G. Marrazza, M. Mascini, Anal. Chim. Acta 609 (2008) 139–159.
[8] T.G. Drummond, M.G. Hill, J.K. Barton, Nat. Biotechnol. 21 (2003) 1192–1199.
[9] M. Hocek, M. Fojta, Chem. Soc. Rev. 40 (2011) 5802–5814.
[10] R. Wang, S. Tombelli, M. Minunni, M.M. Spiriti, M. Mascini, Biosens. Bioelectron. 20 (2004) 967–974.
[11] K. Arora, N. Prabhakar, S. Chand, B.D. Malhotra, Sens. Actuators B: Chem. 126 (2007) 655–663.
[12] T. Berthelot, A. Garcia, X.T. Le, J.E. Morsli, P. Jégou, S. Palacin, P. Viel, Appl. Surf. Sci. 257 (2011) 3538–3546.
[13] Q. Wang, F. Gao, X. Zhang, J. Chen, B. Zhang, Z. Hu, F. Gao, Electrochim. Acta 62 (2012) 250–255.
[14] Z. Li, T. Niu, Z. Zhang, G. Feng, S. Bi, Analyst 137 (2012) 1680–1691.
[15] D.J. Chung, K.C. Kim, S.H. Choi, Appl. Surf. Sci. 257 (2011) 9390–9396.
[16] F. Li, W. Chen, P. Dong, S. Zhang, Biosens. Bioelectron. 24 (2009) 2160–2164.
[17] M. Ligaj, J. Jasnowska, W.G. Musiał, M. Filipiak, Electrochim. Acta 51 (2006) 5193–5198.
[18] M.I. Pividori, A. Merkoci, S. Alegret, Biosens. Bioelectron. 15 (2000) 291–303.
[19] N. Wei, J. Chen, J. Zhang, K. Wang, X. Xu, J. Lin, G. Li, X. Lin, Y. Chen, Talanta 78 (2009) 1227–1234.
[20] H. Gao, X. Qi, Y. Chen, W. Sun, Anal. Chim. Acta 704 (2011) 133–138.
[21] Q. Wang, J. Ni, F. Gao, B. Zhang, S. Li, K. Jiao, J. Bioact. Compat. Polym. 27 (2012) 278–292.
[22] J. Chen, J. Zhang, K. Wang, X. Lin, L. Huang, G. Chen, Anal. Chem. 80 (2008) 8028–8034.
[23] Y.W. Hu, T. Yang, X.X. Wang, K. Jiao, Chem. Eur. J. 16 (2010) 1992–1999.
[24] T. Nomura, J. Electroanal. Chem. Interfacial Electrochem. 139 (1982) 97–104.
[25] A.T. Mubarak, A.A. Mohamed, K.F. Fawy, A.S. Al-Shihry, Talanta 71 (2007) 632–638.
[26] E.L.C. Silveira, L.B. de Caland, M. Tubino, Fuel 90 (2011) 3485–3488.
[27] H. Bhandari, V. Bansal, V. Choudhary, S.K. Dhawan, Polym. Int. 58 (2009) 489–502.
[28] G. Ćirić-Marjanovića, M. Trchováb, P. Matějkac, P. Hollerb, B. Marjanovićd, I. Juraniće, React. Funct. Polym. 66 (2006) 1670–1683.
[29] B. Barbier, J. Pinson, G. Desarmot, M. Sanchez, J. Electrochem. Soc. 137 (1990) 1757–1764.
[30] A.A. Schilt, Analytical Applications of 1,10-Phenanthroline and Related Compounds, first ed., Pergamon Press, Oxford and New York, 1969.
[31] A.B. Steel, T.M. Herne, M.J. Tarlov, Anal. Chem. 70 (1998) 4670–4677.
[32] J. Zhang, S. Song, L. Zhang, L. Wang, H. Wu, D. Pan, C. Fan, J. Am. Chem. Soc. 128 (2006) 8575–8580.
[33] A.J. Downard, A. Mohamed, Electroanalysis 11 (1999) 418–423.
[34] O.Y.F. Henry, A.D. Mehdi, S. Kirwan, J.L.A. Sanchez, C.K. O'Sullivan, Macromol. Rapid Commun. 32 (2011) 1405–1410.
[35] V. Vamvakaki, N.A. Chaniotakis, Electroanalysis 20 (2008) 1845–1850.
[36] E. Sabatani, I. Rubinstein, J. Phys. Chem. 91 (1987) 6663–6669.
[37] J. Wang, S. Zhang, Y. Zhang, Anal. Biochem. 396 (2010) 304–309.
[38] A. Andreu, J.W. Merkert, L.A. Lecaros, B.L. Broglin, J.T. Brazell, M. El-Kouedi, Sens. Actuators B: Chem. 114 (2006) 1116–1120.
[39] F. Li, W. Chen, S. Zhang, Biosens. Bioelectron. 24 (2008) 781–786.
[40] K.M. Millan, S.R. Mikkelsen, Anal. Chem. 65 (1993) 2317–2323.